ORIGINAL ARTICLE

2-Benzamido-*N*-(1*H*-benzo[*d*]imidazol-2-yl)thiazole-4-carboxamide derivatives as potent inhibitors of CK1δ/ε

**Joachim Bischof · Johann Leban · Mirko Zaja ·
Arnhild Grothey · Barbara Radunsky · Olaf Othersen ·
Stefan Strobl · Daniel Vitt · Uwe Knippschild**

Abstract In this study we identified two heterocyclic compounds (**5** and **6**) as potent and specific inhibitors of CK1δ (IC$_{50}$ = 0.040 and 0.042 μM, respectively). Whereas compound **5** exhibited fivefold higher affinity towards CK1δ than to CK1ε (IC$_{50}$ CK1ε = 0.199 μM), compound **6** also inhibited CK1ε (IC$_{50}$ = 0.0326 μM) in the same range as CK1δ. Selected compound **5** was screened over 442 kinases identifying **5** as a highly potent and selective inhibitor of CK1δ. X-ray analysis of **5** bound to CK1δ demonstrated its binding mode. In addition, characterization of **5** and **6** in a cell biological approach revealed the ability of both compounds to inhibit proliferation of tumor cell lines in a dose and cell line specific manner. In summary, our optimizations lead to the development of new highly selective CK1δ and ε specific inhibitors with biological activity.

Keywords CK1δ · CK1ε · Phosphorylation · Small molecule inhibitor · Crystal structure · MTT · FACS

J. Bischof · A. Grothey · B. Radunsky · U. Knippschild (✉)
Department of General, Visceral and Transplantation Surgery,
Surgery Centre, University of Ulm, Steinhövel Str. 9,
89075 Ulm, Germany
e-mail: uwe.knippschild@uniklinik-ulm.de

J. Leban (✉) · M. Zaja · O. Othersen · S. Strobl · D. Vitt
4SC AG, Am Klopferspitz 19a,
82152 Planegg-Martinsried, Germany
e-mail: johan.leban@4sc.com

Present Address:
A. Grothey
Division of Surgery, Oncology, Reproductive Biology
and Anaesthetics Hammersmith Campus, Imperial College,
Cyclotron Building, 5th Floor, London W12 0NN, UK

Introduction

Protein kinases in general represent attractive targets for drug development. Recently, interest in specifically targeting members of the casein kinase 1 (CK1) family, a highly conserved ubiquitously expressed serine/threonine protein kinase family, has increased enormously (Knippschild et al. 2005a). The seven mammalian isoforms CK1α, β, γ$_1$, γ$_2$, γ$_3$, δ and ε and their various splice variants are all highly conserved within their kinase domains (∼290 residues), but differ significantly within their regulatory N-terminal and C-terminal domains. CK1 isoforms can be regulated by inhibitory autophosphorylation mainly occurring within their C-terminal domains, site-specific phosphorylation mediated by cellular kinases, dephosphorylation of autophosphorylation sites, cleavage of the C-terminal domain, and subcellular compartmentalization (Giamas et al. 2007; Knippschild et al. 2005a). CK1 isoforms phosphorylate many different substrates bearing either a canonical or a non-canonical consensus sequence. They are involved in the regulation of many different cellular processes such as canonical Wnt signaling, DNA damage response, cell cycle progression, apoptosis and chromosome segregation (Cheong and Virshup 2010; Price 2006; Knippschild et al. 2005a, b). Since deregulation of CK1 isoforms have been linked to the development of various types of disorders such as cancer (CK1α/γ/δ/ε), neurodegenerative diseases (CK1δ), and inflammatory disorders (CK1α/δ/ε), the use of CK1 (isoform)-specific inhibitors may have therapeutic potential in the cure of these diseases (Gill et al. 2007; Knippschild et al. 2005a; Lin and Peng 2006; Perez et al. 2010).

So far, several CK1-specific inhibitors have been identified, among them IC261 and D4476 (Mashhoon et al. 2000; Rena et al. 2004). However, permeability to the cell

membrane for most available CK1 inhibitors is weak, and their use in vivo restricted. Therefore, efforts are ongoing to identify new potential CK1-specific inhibitors with IC_{50} values in the low nanomolar range which can be used in pharmacological studies and might be effective as therapeutic drugs.

Previously we identified piperidinyl-thiazoles as inhibitors of nuclear factor kappa B (NFκB) (Leban et al. 2007). The well-characterized NFκB is a key player in the signal transduction of severe diseases such as muscular dystrophy, obesity, atherosclerosis, cystic fibrosis, arthritis, Crohn's disease, sepsis, rheumatic disease and cancer (Baghdiguian et al. 1999; Li et al. 2008; Peterson and Guttridge 2008; Bamborough et al. 2010; Demer and Tintut 2011; Nichols et al. 2008; Criswell 2010; Li et al. 2009; Wei and Feng 2010; Gil et al. 2007).When we deleted the piperidinyl residue the compound series described here was obtained. This series exhibited only modest NFκB inhibitory activity (data not shown) but showed significant inhibition of CK1 family members in a selectivity screen comprising 442 eukaryotic protein kinases.

Materials and methods

Intermediate synthesis

Ethyl 2-(2-(trifluoromethoxy)benzamido)thiazole-4-carboxylate

To a solution of ethyl 2-aminothiazole-4-carboxylate (12 g, 70 mmol, 1 eq.) in dry THF (300 ml) *N,N*-diisopropylethylamine (250 ml, 209 mmol, 3 eq.) was added. A solution of 2-(trifluoromethoxy)-benzoyl chloride (19 g, 84 mmol, 1.2 eq.) in THF (50 ml) was added dropwise at 0°C. The reaction mixture was stirred for 24 h at room temperature. Water (50 ml) was added and THF was removed under reduced pressure. The residue was extracted with DCM. The organic layer was dried over MgSO$_4$, filtered and concentrated under reduced pressure. The residue was purified by flash column chromatography on silica gel (PE/EtOAc 80:20). The product was obtained as a white solid (12 g, 33 mmol, 48% yield).

^{1}H NMR (400 MHz, DMSO-d$_6$): δ (ppm) = 1.30 (t, *J* = 7.1 Hz, 3H), 4.29 (q, *J* = 7.1 Hz, 2H), 7.49–7.59 (m, 2H), 7.71 (dt, *J* = 7.8, 1.7 Hz, 1H), 7.79 (dd, *J* = 7.79, 1.7 Hz, 1H), 8.14 (s, 1H), 13.11 (bs, 1H).

2-(2-(Trifluoromethoxy)benzamido)thiazole-4-carboxylic acid

Ethyl 2-(2-(trifluoromethoxy)benzamido)thiazole-4-carboxylate (10 g, 28 mmol, 1 eq.) was dissolved in THF (20 ml) and an aqueous 2 M NaOH solution (110 ml) was added at room temperature. The reaction mixture was stirred for 24 h at room temperature. THF was removed under reduced pressure. The residual aqueous phase was acidified to pH 1–2 using a 15% aqueous HCl solution. The precipitate was collected by filtration, washed with water and dried. The product was obtained as a white solid (9.3 g, 28 mmol, quant.).

^{1}H NMR (400 MHz, DMSO-d$_6$): δ (ppm) = 7.49–7.59 (m, 2H), 7.70 (dt, *J* = 7.8, 1.7 Hz, 1H), 7.79 (dd, *J* = 7.79, 1.7 Hz, 1H), 8.06 (s, 1H), 13.01 (bs, 2H).

Final compounds

Methyl 2-(2-(2-(trifluoromethoxy)benzamido)-thiazole-4-carboxamido)-1H-benzo[d]imidazole-5-carboxylate (*1*)

N,N-diisopropylethylamine (6.1 g, 47.1 mmol) was added dropwise to a solution of 2-(2-(trifluoromethoxy)benzamido)thiazole-4-carboxylic acid (5.2 g, 15.7 mmol) in 50 ml DMF. Then HBTU (6.2 g, 16.5 mmol) was added at 0°C and the reaction mixture was stirred for 25 min. Methyl 2-amino-1*H*-benzo[*d*]imidazole-5-carboxylate (3.0 g, 15.7 mmol) was added portionwise and the reaction mixture was stirred for 16 h. Water (250 ml) was added and the reaction mixture was stirred for 20 min. Then a saturated aqueous NaHCO$_3$ solution (20 ml) was added and the mixture was stirred for further 20 min. The suspension was filtered and the solid was washed with water and dried. The residue was purified by flash column chromatography on silica (DCM/MeOH 100:0–100:5). All product fractions were collected and concentrated under reduced pressure. The residue was washed with cold MeOH and dried. The product was obtained as a white solid (2.4 g, 4.7 mmol, 30% yield).

^{1}H NMR (400 MHz, DMSO-d$_6$): δ (ppm) = 3.86 (s, 3H), 7.48–7.64 (m, 3H), 7.73 (dt, *J* = 7.9, 1.5 Hz, 1H), 7.76–7.88 (m, 2H), 8.12 (s, 1H), 8.36 (s, 1H), 11.42 (bs, 1H), 12.54 (bs, 1H), 13.10 (bs, 1H).

N-(5-(Methylsulfonyl)-1H-benzo[d]imidazol-2-yl)-2-(2-(trifluoromethoxy)benzamido)thiazole-4-carboxamide (*2*)

2-(2-(Trifluoromethoxy)benzamido)thiazole-4-carboxylic acid (0.30 g, 0,9 mmol), 5-(methylsulfonyl)-1*H*-benzo[*d*]-imidazol-2-amine (0.19 g, 0.9 mmol), HBTU (0.34 g, 0.9 mmol) and DMAP (11 mg, 0.09 mmol) were dissolved in DMF (20 ml). The reaction mixture was stirred for 16 h at 60°C. The reaction mixture was diluted with EtOAc and washed with a saturated aqueous NaHCO$_3$ solution and a 5% aqueous citric acid solution. The organic phase was dried over MgSO$_4$ filtered and concentrated under reduced pressure. The residue was purified by preparative HPLC/MS. Only the pure fractions were collected and

concentrated under reduced pressure. The product was obtained as a white solid (16 mg, 0.03 mmol, 3% yield).

N-(1-Methyl-1H-benzo[d]imidazol-2-yl)-2-(2-(trifluoromethoxy)benz-amido)thiazole-4-carboxamide (3)

To a solution of 2-(2-(trifluoromethoxy)benzamido)thiazole-4-carboxylic acid (3.2 g, 9.7 mmol) in DMF (45 ml) HBTU (3.9 g, 10.2 mmol) was added portionwise at 0°C, followed by dropwise addition of N,N-diisopropylethylamine (3.8 g, 29.1 mmol). The cooling bath was removed and the reaction mixture was stirred for 10 min. 1-methyl-1H-benzo[d]imidazol-2-amine (1.5 g, 10.2 mmol) was added portionwise and the reaction mixture was stirred at room temperature for 16 h. An aqueous 1 M NaOH solution was added and the reaction mixture was stirred for 15 min. The mixture was diluted with water (10 ml) and extracted with MTBE. The organic extracts were extracted with an aqueous 1 M NaOH solution. The combined aqueous phases were acidified to pH 1–2 using conc. HCl. The formed precipitate was filtered and washed with PE and dried. The product was obtained as a white solid (3.0 g, 6.5 mmol, 64% yield).

^{1}H NMR (400 MHz, DMSO-d_6): δ (ppm) = 3.69 (s, 3H), 7.16-7.31 (m, 2H), 7.41–7.60 (m, 4H), 7.64–7.75 (m, 1H), 7.76–7.85 (m, 1H), 8.11 (s, 1H), 12.56 (bs, 1H), 13.00 (bs, 1H).

2-(Isonicotinamido)-N-(6-(trifluoromethyl)-1H-benzo[d]imidazol-2-yl)thiazole-4-carboxamide (4)

To a solution of 2-(isonicotinamido)thiazole-4-carboxylic acid (0.4 g, 1.6 mmol) and 6-(trifluoromethyl)-1H-benzo[d]-imidazol-2-amine (0.3 g, 1.6 mmol) in DMF (5 ml) HBTU (0.6 g, 1.6 mmol) and N,N-diisopropylethylamine (0.3 ml, 0.2 g, 1.6 mmol) were added. The reaction mixture was stirred at room temperature for 16 h. All volatiles were removed under reduced pressure. The residue was suspended in water and the solid filtered off. The crude product was purified by preparative HPLC/MS. Only the pure fractions were collected and concentrated under reduced pressure. The product was obtained as a white solid (12 mg, 0.03 mmol, 2% yield).

2-(2-(Trifluoromethoxy)benzamido)-N-(6-(trifluoromethyl)-1H-benzo[d]imidazol-2-yl)thiazole-4-carboxamide (5)

To a solution of 2-(2-(trifluoromethoxy)benzamido)thiazole-4-carboxylic acid (3.4 g, 10.4 mmol) in DMF (50 ml) N,N-diisopropylethylamine (4.0 g, 31.1 mmol) was added dropwise at 0°C followed by the addition of HBTU (4.1 g, 10.9 mmol). After stirring for 15 min at 0°C 6-(trifluoromethyl)-1H-benzo[d]imidazol-2-amine (2.1 g, 10.4 mmol) was added portionwise. The reaction mixture was stirred at room temperature for 16 h. All volatiles were removed under reduced pressure. The residue was dissolved in MTBE and washed with an aqueous 5% citric acid solution. The organic phase was extracted with an aqueous 1 M NaOH solution. The combined aqueous phases were acidified to pH 1–2 using conc. HCl. The formed precipitate was filtered and washed with PE and dried. The product was obtained as a white solid (1.5 g, 2.9 mmol, 28% yield).

^{1}H NMR (400 MHz, DMSO-d_6): δ (ppm) = 7.42–7.49 (m, 1H), 7.51–7.61 (m, 2H), 7.63–7.76 (m, 2H), 7.79–7.86 (m, 1H), 8.38 (s, 1H), 11.38 (bs, 1H), 12.60 (bs, 1H), 13.11 (bs, 1H).

N-(5-Chloro-6-fluoro-1H-benzo[d]imidazol-2-yl)-2-(2-(trifluoromethoxy) benzamido)thiazole-4-carboxamide (6)

To a solution of 2-(2-trifluoromethoxy-benzoylamino)-thiazole-4-carboxylic acid (3.0 g, 9.0 mmol) in DMF 5-chloro-6-fluoro-1H-benzo[d]imidazol-2-amine (1.8 g, 9.5 mmol) and N,N-diisopropylethylamine (4.5 ml, 3.5 g, 27.1 mmol) were added. The reaction mixture was cooled to 0°C and HBTU (3.6 g, 9.5 mmol) was added portionwise. The reaction mixture was stirred at room temperature for 16 h. All volatiles were removed under reduced pressure. The residue was washed with a saturated aqueous NaHCO$_3$ solution, a 5% aqueous citric acid solution and MeOH. The residue was purified by flash column chromatography on silica (DCM/MeOH 95:5). The product was obtained as a white solid (1.1 g, 2.2 mmol, 24% yield).

^{1}H NMR (400 MHz, DMSO-d_6): δ (ppm) = 7.47 (d, J = 9.75 Hz, 1H), 7.51–7.60 (m, 2H), 7.63 (d, J = 6.87 Hz, 1H), 7.73 (dt, J = 7.86, 1.68 Hz, 1H), 7.82 (dd, J = 7.56, 1.59 Hz, 1H), 8.37 (s, 1H), 11.24 (bs, 1H), 12.46 (bs, 1H), 13.10 (bs, 1H).

2-(Furan-2-carboxamido)-N-(6-(trifluoromethyl)-1H-benzo[d]imidazol-2-yl)thiazole-4-carboxamide (7)

To a solution of 2-(furan-2-carboxamido)thiazole-4-carboxylic acid (80 mg, 0.3 mmol) and 6-(trifluoromethyl)-1H-benzo[d]imidazol-2-amine (68 mg, 0.3 mmol) HBTU (127 mg, 0.3 mmol) and N,N-diisopropylethylamine (117 μl, 0.7 mmol) were added and the reaction mixture was stirred at 85°C for 16 h. The reaction mixture was poured into ice water and the formed precipitate filtered off, washed with water and dried. The product was obtained as a white solid (50 mg, 0.1 mmol, 35% yield).

N-(1H-Benzo[d]imidazol-2-yl)-2-(2-(trifluoromethoxy)benzamido)thiazole-4-carboxamide (8)

To a solution of 2-(2-(trifluoromethoxy)benzamido)thiazole-4-carboxylic acid (2.0 g, 6.0 mmol) in DMF (15 ml) N,N-diisopropylethylamine (2.3 g, 18.1 mmol) was added

dropwise. The reaction mixture was cooled to 0°C and HBTU (2.4 g, 6.3 mmol) was added portionwise. The reaction mixture was stirred at room temperature for 1 h. Then 1*H*-benzo[*d*]imidazol-2-amine (0.8 g, 6.3 mmol) was added portionwise and the reaction mixture was stirred at room temperature for 48 h. An aqueous 1 M NaOH solution (5 ml) was added and the reaction mixture was stirred for 15 min. The mixture was diluted with water (10 ml) and extracted with MTBE. The organic extracts were extracted with an aqueous 1 M NaOH solution. The combined aqueous phases were acidified to pH 1–2 using conc. HCl. The formed precipitate was filtered and washed with PE and dried. The product was obtained as a white solid (1.1 g, 2.4 mmol, 41% yield).

^{1}H NMR (400 MHz, DMSO-d$_6$): δ (ppm) = 7.09–7.17 (m, 2H), 7.44–7.51 (m, 2H), 7.52–7.61 (m, 2H), 7.73 (dt, J = 7.87, 1.77 Hz, 1H), 7.82 (dd, J = 7.58, 1.61 Hz, 1H), 8.27 (s, 1H), 11.91 (bs, 2H), 13.05 (bs, 1H).

2-(2-Trifluoromethoxy-benzoylamino)-thiazole-4-carboxylic acid benzothiazol-2-ylamide (9)

2-(2-(Trifluoromethoxy)benzamido)thiazole-4-carboxylic acid (0.1 g, 0.3 mmol) was dissolved in DMF (3 ml) and *N,N*-diisopropylethylamine (39 mg, 0.3 mmol) was added. The reaction mixture was stirred for 2 min and HBTU (0.1 g, 0.3 mmol) and benzo[*d*]thiazol-2-amine (45 mg, 0.3 mmol) were added. The reaction mixture was stirred at 70°C for 16 h. All volatiles were removed under reduced pressure. The residue was dissolved in EtOAc and washed with a 5% aqueous citric acid solution, a saturated aqueous NaHCO$_3$ solution and water. The organic phase was dried over MgSO$_4$, filtered and concentrated under reduced pressure. The residue was purified by preparative TLC (DCM/MeOH 95:5). The product was obtained as a white solid (33 mg, 0.07 mmol, 24% yield).

^{1}H NMR (400 MHz, DMSO-d$_6$): δ (ppm) = 7.34 (dt, J = 8.10, 1.14 Hz), 7.47 (dt, J = 8.19, 1.23 Hz, 1H), 7.51–7.61 (m, 2H), 7.73 (dt, J = 7.95, 1.77 Hz, 1H), 7.79 (d, J = 7.98 Hz, 1H), 7.82 (dd, J = 7.59, 1.62 Hz, 1H), 8.02 (d, J = 7.32 Hz, 1H), 8.44 (s, 1H), 12.07 (bs, 1H), 13.08 (bs, 1H).

N-(Benzo[d]oxazol-2-yl)-2-(2-(trifluoromethoxy)benzamido) thiazole-4-carboxamide (10)

To a solution of 2-(2-(trifluoromethoxy)benzamido)thiazole-4-carboxylic acid (1.4 g, 4.2 mmol) in DMF (50 ml) *N,N*-diisopropylethylamine (1.6 g, 12.5 mmol) was added dropwise. The reaction mixture was cooled to 0°C and HBTU (1.7 g, 4.4 mmol) was added portionwise. The reaction mixture was stirred at room temperature for 15 min. Then benzo[*d*]oxazol-2-amine (0.6 g, 4.4 mmol)

was added portionwise and the reaction mixture was stirred at room temperature for 16 h.

All volatiles were removed under reduced pressure. The residue was dissolved in MTBE and washed with an aqueous 5% citric acid solution and a saturated aqueous NaHCO$_3$ solution. The organic phase was dried over MgSO$_4$, filtered and concentrated under reduced pressure. The residue was purified by flash column chromatography on silica (DCM/MeOH 100:0 to 99:1). The crude product was dissolved in a small amount MeOH and water was added. The precipitate was dried to afford the product as a white solid (750 mg, 1.7 mmol, 40% yield).

^{1}H NMR (400 MHz, DMSO-d$_6$): δ (ppm) = 7.27–7.39 (m, 2H), 7.50–7.76 (m, 5H), 7.81 (d, J = 7.59 Hz, 1H), 8.30 (s, 1H), 11.48 (bs, 1H), 13.08 (bs, 1H).

Plasmids

CK1δTV1 and 2 (transcription variants 1 and 2) were PCR amplified from mouse cDNA (5′-primer TV1 and 2: 5′-G GATCCATGGAGCTGAGGGTCGGGAATAG-3′, 3′-primer TV1: 5′-GGATCCTCATCGGTGCACGACAGACT GA-3′, 3′-primer TV2: 5′-GGATCCCTACTTGCCGTGG TGTTCGAAA-3′) and cloned into pcDNA3.1/V5-His© TOPO® TA cloning vector (Invitrogen, Karlsruhe, Germany) before being subcloned into pGEX-2T expression vector via *Bam*HI to generate plasmids pGEX-2T-mouse CK1δTV1 (FP1170) and pGEX-2T-mouse CK1δTV2 (FP1171).

For the expression of wt rat CK1δ and rat CK1δ^{M82F} as glutathione S-transferase fusion proteins the plasmids pGEX-2T-CK1δ (FP449) (Knippschild et al. 1997) and pGEX-2T-CK1δ^{M82F} (FP1153) (Peifer et al. 2009) were used.

Plasmid pGEX-2T-mouse p53$^{1–64}$ was used to express GST-mouse p53$^{1–64}$ (FP267) which was used as substrate in in vitro kinase reactions (Milne et al. 1992).

Overexpression and purification of glutathione S-transferase fusion proteins

Expression and purification of the GST-fusion proteins GST-mouse p53$^{1–64}$ (FP267), GST-rat CK1δ (FP449), GST-rat CK1δ^{M82F} (FP1153), GST-mouse CK1δTV1 (FP1170), and GST-mouse CK1δTV2 (FP1171) was carried out as described elsewhere (Wolff et al. 2005). Expression of fusion proteins FP1170 and 1171 was either performed at 37°C for 2 h, or at 15°C for 14 h. FP449 and FP1153 were always expressed at 15°C for 14 h.

In vitro kinase assays

In vitro kinase assays were carried out in the presence of various potential inhibitors of CK1δ at an ATP concentration of 0.01 mM and dimethyl sulfoxide (DMSO)

solvent control as described previously (Knippschild et al. 1996). Where indicated higher ATP concentrations (0.05, 0.1, 0.25 and 0.5 mM) were used. The fusion protein GST-mouse $p53^{1-64}$ (FP267) was used as substrate. Recombinant CK1δ kinase domain (CK1δkd, NEB, Frankfurt am Main, Germany), GST-rat CK1δ (FP449), GST-rat CK1δ^{M82F} (FP1153), GST-mouse CK1δTV1, GST-mouse CK1δTV2 and recombinant human CK1ε (Invitrogen, Karlsruhe, Germany) were used as sources of enzyme. Phosphorylated proteins were separated by SDS-PAGE and the protein bands were visualized on dried gels by autoradiography. The phosphorylated protein bands were excised and quantified by Cherenkov counting.

Phosphopeptide analysis

Phosphopeptide analysis of in vitro labeled proteins was carried out as described previously (Wolff et al. 2005).

KINOMEscan: high-throughput kinase selectivity profiling

KINOME*scan*™ was performed to determine binding constants of coumpound **5** to 442 eukaryotic kinases by Ambit Biosciences Cooperation, San Diego, USA.

X-ray analyses

Crelux (CRELUX GmbH, Martinsried, Germany) produced co-crystals of a human truncated mutant casein kinase 1 δ (CK1δ$^{1-316, R13N}$) with compound **5** that diffract to 1.7 Å resolutions at the ESRF synchrotron radiation source and determined the X-ray structure.

Crystals were obtained using sitting drop vapor diffusion setups. The diluted protein solution (1 mg/ml) was incubated at room temperature for 2 h with 15 mM of compound **5** and then concentrated to 13.5 mg/ml. 0.4 μl of protein solution (13.5 mg/ml in 50 mM HEPES, 200 mM NaCl, 1 mM EDTA, 1 mM DTT, 5 mM β-OG, pH 7.5) was mixed with 0.4 μl of reservoir solution (0.1 M NaCl, 1.4 M $(NH_4)_2SO_4$, 0.1 M bis–tris, pH 5.8) and equilibrated over 60 μl of reservoir solution. Crystals appeared after 1–3 days.

The structure was determined by molecular replacement using the published CK1δ structure (PDB accession code 1CKI) as search model followed up by refinement of this model with REFMAC5 (Collaborative Computational Project 1994; Murshudov et al. 1996). Several rounds of alternating manual rebuilding and refinement resulted in the final model.

Modeling M82F mutant and docking

Based on the X-ray structure of human CK1δ$^{1-316, R13N}$ with compound **5** the gatekeeper methionine 82 was mutated to phenylalanine 82 and energetically minimized using MOE (MOE (The Molecular Operating Environment) Version 2010.10, software available from Chemical Computing Group Inc. http://www.chemcomp.com).

Both nitrogen-protonated benzimidazol-tautomers [1H] and [3H] of compounds **4–6** were docked without crystal water or co-ligands into the wild type CK1δ and M82F mutant. The best-scored docking solutions and corresponding protein were fully optimized in MOE and rescored. The [3H] tautomers were only used in docking.

Cell lines

Frwt648 cells [generated by SV40-transformation of F111 cells; (Hinzpeter and Deppert 1987)] and mKSA cells [SV40-transformed Balb/c fibroblasts; (Kit et al. 1969)] were grown in Dulbecco's modified Eagle's medium (DMEM) supplemented with 5% fetal calf serum (FCS; Biochrom, Berlin, Germany). The fibrosarcoma cell line HT1080 (Rasheed et al. 1974) was grown in DMEM containing 10% FCS and 2 mM glutamine while both the prostate cancer cell line DU-145 (Stone et al. 1978) and the ovary tissue cancer cell line OVCAR-3 (Hamilton et al. 1983) were maintained in RPMI-1640 supplemented with 10% FCS. The pancreatic cancer cell line Colo357 (Morgan et al. 1980) was grown in DMEM/RPMI (1:1) and the colon adenocarcinoma cell line SW480 (Leibovitz et al. 1976) in Leibovitz L-15 medium, both containing 10% FCS and 2 mM glutamine. All media were supplemented with 100 U/ml penicillin and 100 μg/ml streptomycin (Gibco, Karlsruhe, Germany) and all cell lines were grown at 37°C in a humidified 5% carbon dioxide atmosphere.

Flow cytometry and cell cycle analysis

Subconfluent Frwt648, mKSA, Colo357, OVCAR-3, HT1080, DU-145 and SW480 cells were treated with 2 or 4 μM of compounds **5** or **6** for 48 h. Untreated and DMSO treated cells served as control. Cells were harvested, washed once with phosphate-buffered saline (PBS), and prepared for cell cycle analysis using the "Cycle Test Plus Kit" (BD, San Jose, USA). Cell cycle profiles were obtained using a FACScan flow cytometer and CellQuest software (BD Biosciences, San Jose, USA).

Results

Biological activity of new identified compounds

Compounds **1–10** (Table 1) were initially assayed for their biological activity against CK1δkd and CK1ε at a concentration of 10 μM ATP (Fig. 1a, b). Compounds **4, 5** and

6, which showed significant inhibition of CK1δkd and CK1ε in these assays were further characterized for their IC$_{50}$ values against CK1δkd, GST-rat CK1δ, GST-mouse CK1δTV1, GST-mouse CK1δTV2 and human CK1ε (Table 2). Differences in the IC$_{50}$ values of compounds **4**, **5** and **6** against CK1δ transcription variants could be due to their differences in amino acid composition and the degree of site-specific phosphorylation within their C-terminal regulatory domains. This prediction is underlined by two dimensional phosphopeptide analyses showing quantitative and qualitative differences in the degree of phosphorylation of CK1δTV1 and CK1δTV2 (Fig. 2). Furthermore, induction of recombinant CK1δ transcription variants in bacteria at different temperatures influences its phosphorylation status, activity and sensibility towards small molecule inhibitors (Fig. 3). CK1δ transcription variants induced at 15°C for 14 h are more active and incorporate more radioactive phosphate in the substrate than CK1δ transcription variants induced at 37°C for 2 h (Fig. 3a). Lower degree of phosphorylation of both transcription variants increases the ability of compound **5** to inhibit substrate phosphorylation of both transcription variants indicated by their 1.5- to 2-fold lower IC$_{50}$ values (Fig. 3b).

Selectivity profiling of compound 5 in a panel of 442 protein kinases

In order to investigate the specificity of compound **5** its ability to inhibit other kinases at a concentration of 10 μM a KINOME*scan*^{TM} (KINOMEscan, San Diego, USA) with a panel of 442 protein kinases was performed (Fig. 4). In this assay CK1 isoforms were potentially inhibited by compound **5** (CSNK1E 0.35%, CSNK1D 2% and CSNK1A1 3% remaining kinase activity relative to controls), while most kinases were not affected significantly. However, in the presence of compound **5** (10 μM) the kinase activities of few kinases were similarly low, among them CLK1 (2.6%), DYRK1A (4.1%), CLK4 (7.2%), DYRK1B (6.6%), and PIP5K2C (9.6%).

Binding mode of compound 5 to CK1δ

The tertiary structure of the protein is well conserved in comparison with 1CKI. The DFG-motiv exhibits the 'in'-conformation (Pargellis et al. 2002). Compound **5** binds to the ATP-site as depicted in Fig. 5. The sidechain conformation of gatekeeper methionine 82 is more compact to
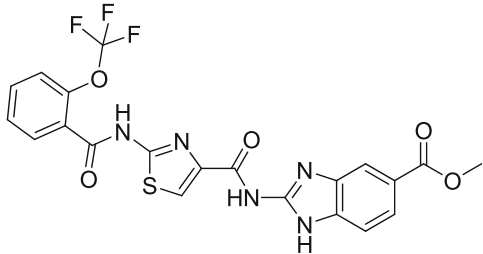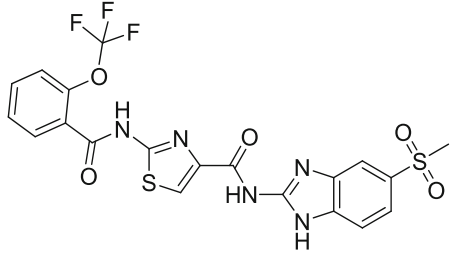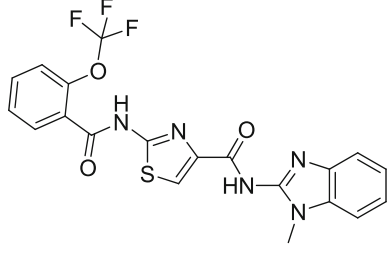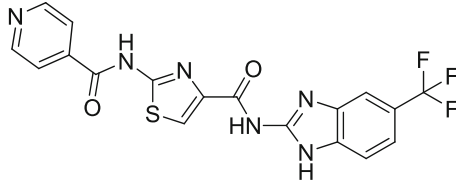
Table 1 CK1 inhibitors
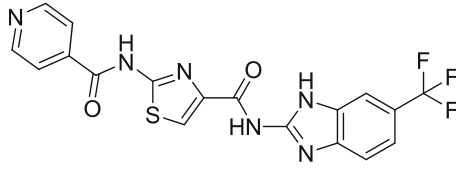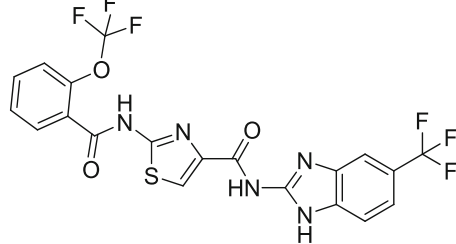
Structure	Compound number
	1
	2
	3
	4
	4b (only for docking)
	5

Table 1 continued

Structure	Compound number
	5b (only for docking)
	6
	6b (only for docking)
	7
	8
	9

Table 1 continued

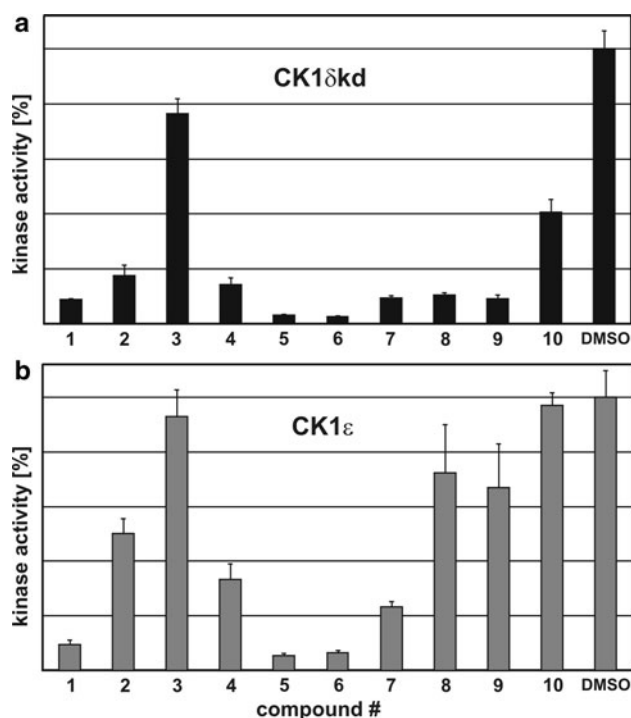| Structure	Compound number
	10

Fig. 1 Effect of various inhibitor compounds on CK1δkd and CK1ε kinase activity. Inhibitor compounds **1–10** were screened in in vitro kinase assays for biological activity to inhibit CK1δkd (**a**) or CK1ε (**b**). Each inhibitor was used at a concentration of 10 μM. Results are shown as normalized bar graph

accommodate the trifluoromethyl-group but no deeper/ selectivity pocket is opened. Hinge residues leucine 84 and leucine 85 are hydrogen bonded via the backbone carbonyl to NH and the backbone nitrogen to the imidazole nitrogen of compound **5**, respectively. CH/π-bonds are formed for all three aromatic regions of compound **5**. Hydrophobic interactions exist between the trifluoromethoxy-group and

Table 2 Biological activity of heterocyclic compounds **4**, **5** and **6** against CK1δkd, GST-rat CK1δ, GST-mouse CK1δTV1, GST-mouse CK1δTV2 and CK1ε

No.	IC$_{50}$ (μM) CK1δkd	IC$_{50}$ (μM) GST-CK1δ rat	IC$_{50}$ (μM) GST-CK1δ TV1	IC$_{50}$ (μM) GST-CK1δ TV2	IC$_{50}$ (μM) CK1ε
1	0.865 ± 0.14	1.975 ± 0.85	nd	nd	0.496 ± 0.10
2	1.225 ± 0.41	5.189 ± 1.14	nd	nd	nd
3	>	>	nd	nd	nd
4	0.409 ± 0.12	0.326 ± 0.19	0.180 ± 0.03	0.505 ± 0.04	nd
5	0.029 ± 0.01	0.040 ± 0.01	0.022 ± 0.02	0.042 ± 0.02	0.199 ± 0.15
6	0.085 ± 0.01	0.042 ± 0.05	0.048 ± 0.02	0.055 ± 0.02	0.033 ± 0.01
7	0.542 ± 0.05	1.036 ± 0.31	nd	nd	nd
8	1.116 ± 0.19	0.935 ± 0.55	nd	nd	nd
9	0.730 ± 0.11	1.193 ± 0.39	nd	nd	nd
10	0.647 ± 0.04	0.991 ± 0.21	nd	nd	nd

Results are presented as mean ± SD from experiments performed at least in triplicate

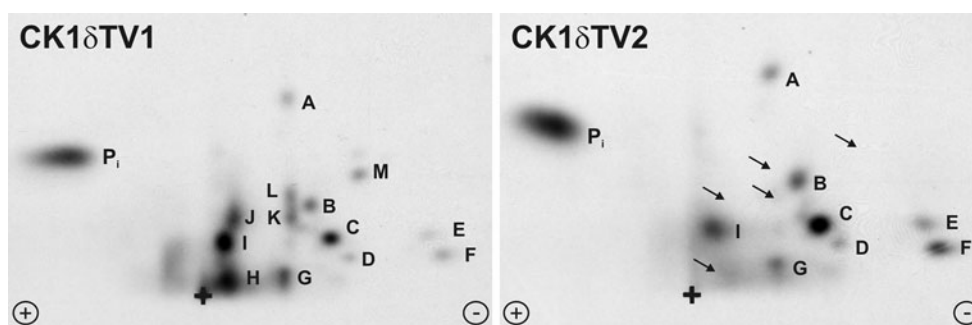>, IC$_{50}$ could not be determined within the range of 10–0.005 μM; *nd*, not determined

Fig. 2 Comparison of the phosphorylation of mouse CK1δTV1 and TV2. Purified GST-mouse CK1δTV1 and GST-mouse CK1δTV2 were autophoshorylated in vitro for 30 min. Phosphorylated proteins were separated by SDS-PAGE, blotted onto PVDF membranes, trypsinized and oxidized. The resulting phosphopeptides were separated in two dimensional analyses by electrophoresis at pH 1.9 and ascending chromatography. Phosphopeptides were labeled with *capital letters*. Phospopeptides *H*, *J*, *K*, *L*, and *M* were only present in CK1δTV1, whereas except *G* and *I* all other phosphopeptides (*A*, *B*, *C*, *D*, *E*, and *F*) of CK1δTV1 were reduced in comparison to those of CK1δTV2

the sidechains of proline 87, leucine 92, phenylalanine 95, leucine 293 and phenylalanine 295. Furthermore, three crystal water molecules are found near compound **5** saturating hydrogen bond functions of the ligand and the protein surface. These water molecules are all solvent exposed and should therefore have no influence on the binding mode.

Compounds 4, 5 and 6 are ATP competitive inhibitors of CK1δ

In order to prove these compounds as ATP competitive inhibitors, **4**, **5** and **6** were tested at their IC$_{50}$ concentrations for the potency to inhibit CK1δkd in the presence of different amounts of ATP (Fig. 6a–c). Since the IC$_{50}$ values increased progressively upon raising the concentration of ATP the ATP competitive properties of all tested compounds were confirmed. This finding underlines and clearly shows that **4**, **5** and **6** are highly potent inhibitors of CK1δ which are able to bind and block kinase activity even in the presence of increased ATP concentrations.

Inhibitory effects of compounds 4, 5 and 6 on GST-wt CK1δ and GST-CK1δ^{M82F}

Previously it has been shown that methionine 82 plays an important role as gatekeeper residue in the docking mode of isoxazoles to the ATP binding pocket since mutation of methionine 82 to phenylalanine blocks binding of this class of CK1δ specific inhibitors (Peifer et al. 2009) while still binding ATP. Therefore, we now analyzed the effects of exchanging methionine 82 to phenylalanine on the ability of compounds **4**, **5** and **6** to inhibit CK1δ activity. In vitro kinase assays were performed in the absence and presence of **4**, **5** and **6** at their determined IC$_{50}$ concentrations using GST-wt CK1δ or GST-CK1δ^{M82F} as the source of enzyme. GST-wt CK1δ activity was clearly decreased in the presence of **4**, **5** and **6**. Interestingly, in comparison with inhibition of GST-wt CK1δ the kinase activity of GST-CK1δ^{M82F} was much more affected in reactions containing compounds **4** or **5**, but similarly or even less affected by compound **6** (Fig. 7). These observations underline the different binding mode of these compounds than that of
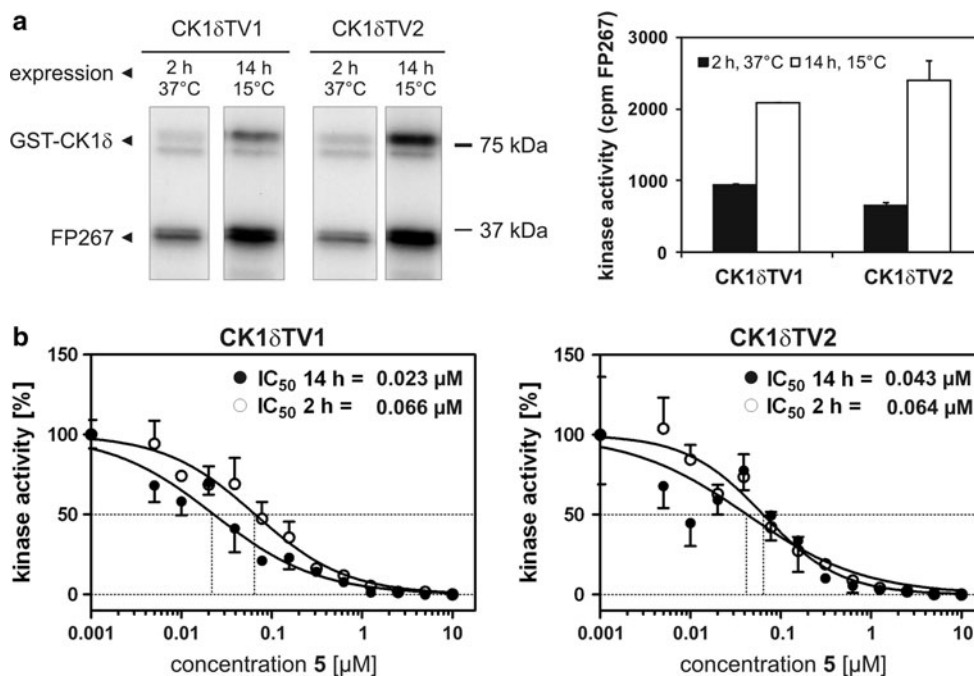
Fig. 3 The degree of phosphorylation influences the activity of CK1δ transcription variants and modulates the inhibitory effects of compound **5**. **a** Comparision of substrate phosphorylation of CK1δ transcription variants induced at 15°C or 37°C. Purified CK1δTV1 and CK1δTV2 either having been induced for 2 h at 37°C or for 14 h at 15°C were used for phosphorylation of GST-mouse p53$^{1-64}$ in vitro. **b** Determination of the inhibitory ability of compound **5** towards CK1δ transcription variants differing in their phosphorylation degree. Compound **5** was tested for its ability to inhibit CK1δTV1 and CK1δTV2 which have either been induced for 2 h at 37°C or for 14 h at 15°C. A high degree of phosphorylation of both CK1δ transcription variants resulted in recuced inhibitory effects of **5** indicated by three- to fourfold higher IC$_{50}$ values

isoxazoles, which address the selectivity pocket, while compounds **4**–**6** do not bind to this region in the active site.

Differences in ligand interaction of compounds **4**, **5** and **6** in wt CK1δ and CK1δ^{M82F}

Docking poses in wt CK1δ and CK1δ^{M82F} align well with the X-ray determined pose of compound **5** in the wild type. Mutation of methionine 82 has nearly no influence on the docking pose, although the cavity for the ligand is marginally reduced. For compounds **4** and **5** the synthesized [1H] benzimidazole tautomers exhibit a better docking score than the [3H] tautomers **4b** and **5b**, whereas the [3H] tautomer **6b** scores better than the synthesized compound **6**. As tautomerism within the assay cannot be excluded, both tautomers for compound **6** were optimized and rescored. Regardless of tautomerism, the NH$_{Leu85}$···N$_{Benzimidazol}$ hydrogen bond is always formed (Fig. 5), resulting in a flip of the benzimidazole ring and thus a different orientation of the attached functional groups. However, in all cases the docking scores for compounds **4** and **5** in CK1δ^{M82F} improve compared to wt CK1δ whereas compounds **6** and **6b** fall off and are thus in accordance with the experimental results (Table 3). The differences can be explained by the π-hydrogen bond between benzimidazole and phenylalanine 82, which is not possible for both tautomers of compound **6**. The necessary hydrogen is substituted with fluorine or chlorine, respectively (Fig. 8).

Efficacy of **5** and **6** in cell culture

Although potent inhibition of CK1δ has been observed for several inhibitor compounds in vitro, these might not necessarily show similar effects in in vivo experiments. In order to identify inhibitors which are able to pass cell membranes and inhibit proliferation of tumor cell lines, a panel of seven cell lines (Frwt648, mKSA, Colo357, OV-CAR-3, HT1080, DU-145 and SW480) was either treated with 2 or 4 μM of compounds **5** or **6** (or with DMSO as a negative control) for 48 h. FACS analyses were performed to compare the effects of both compounds with those of vehicle only (DMSO) with respect to cell viability and cell cycle distribution. Our results indicated that the SV40-transformed Frwt648 and mKSA cell lines are highly sensitive towards treatment with 2 and 4 μM of compounds **5** and **6** (35–98% dead cells; Fig. 9). Similar, but significantly weaker effects could be observed for cell lines HT1080, DU-145 and SW480 after 48 h treatment with

a

KINOMEscan Gene Symbol	%Ctrl @ 10 µM
CLK1	2.6
CLK2	10
CLK3	20
CLK4	7.2
CSNK1A1	3
CSNK1A1L	1
CSNK1D	2
CSNK1E	0.35
CSNK1G2	9.9
CSNK1G3	31
DYRK1A	4.1
DYRK1B	6.6
DYRK2	17
FLT3(D835H)	25
FLT3(D835Y)	10
FLT3(ITD)	24
IRAK3	27
PIP5K2C	9.6
SLK	12
TAOK1	24
TAOK3	20

0 ≤ x < 1   1 ≤ x < 10   10 ≤ x < 35

b compound 5

Fig. 4 Determination of selectivity of compound **5**. In order to determine target selectivity, a panel of 442 protein kinases was screened for inhibition by compound **5** at a concentration of 10 µM. **a** Targets showing less than 35% of control activity in the presence of
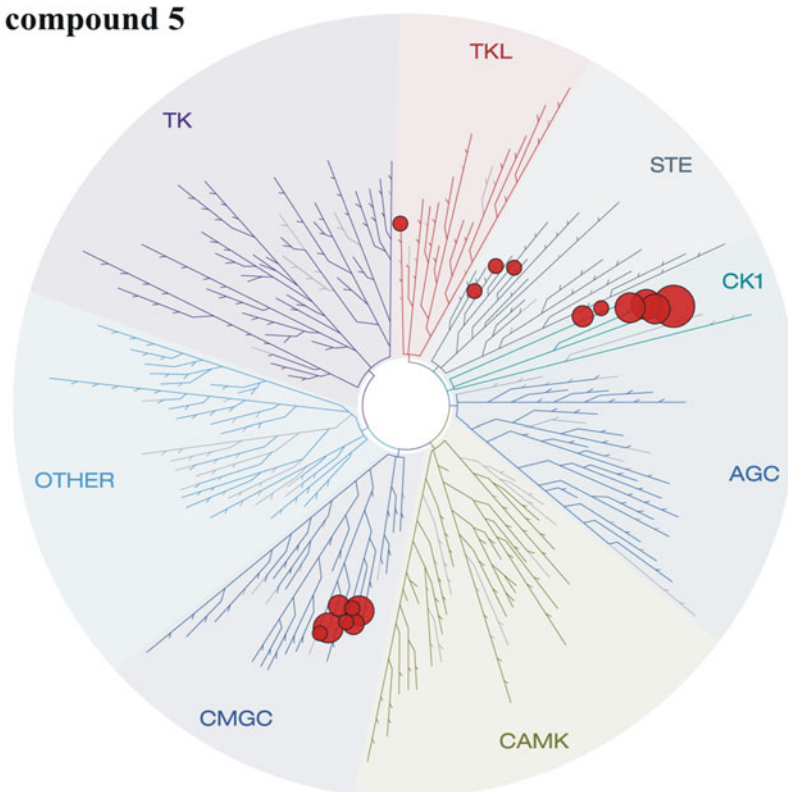
5. **b** Illustration of targets phylogenetic relations listed in (**a**). Image generated using TREE*spot*™ Software Tool and reprinted with permission from KINOME*scan*™, a division of DiscoveRx Corporation, © DISCOVERX CORPORATION 2010
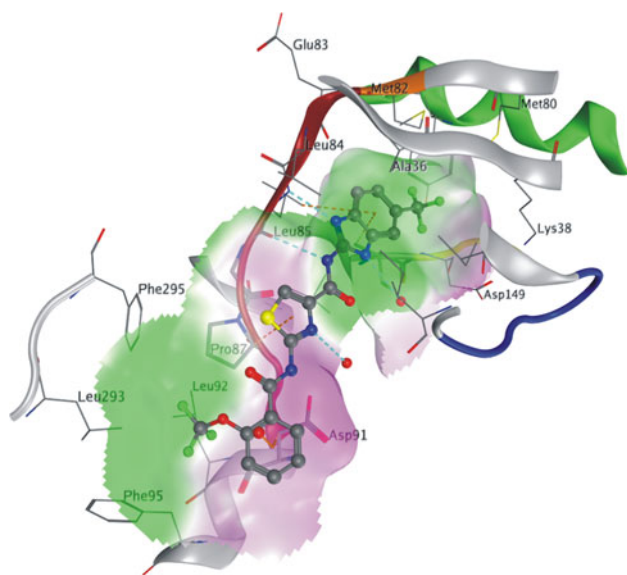

Fig. 5 X-ray structure of **5** in the ATP binding pocket of CK1δ. Residues within 4.5 Å of compound **5** are fully shown, whereas the backbone is visualized in parts, color-coded for the kinase-typical structural elements (αC *green*, gatekeeper *orange*, hinge-region *red*, gylcine-rich loop *blue* and DFG-motif *yellow* (*background*)). The *doted lines* depict hydrogen bonds in cyan for standard and orange for π-hydrogen bonds

compounds **5** and **6** (data not shown). However, no measurement using these three cell lines detected more than 20% of dead cells with DU-145 even being unsusceptible to treatment with compound **5** (data not shown). In addition to the increased amount of dead cells after 48 h treatment of Colo357 cells with compounds **5** and **6**, more cells appeared to be in the G1 phase of the cell cycle (Fig. 9). OVCAR-3 cells were more sensitive to compound **6** in the tested concentrations as 22, and 39%, respectively, of the cells died upon treatment. Treatment of OVCAR-3 cells with compound **5** resulted in a slight increase of cells in the G2 phase of the cell cycle (Fig. 9).

In general, results of this screening show cell line specific differences in the potency of the tested inhibitors to induce apoptosis or cell cycle arrest.

Discussion

Recently, it has become practice to screen cellular pathways in whole cell systems with chemical libraries and then find the cellular target by proteomics or biochemical methods. We have screened for NFκB inhibitors and found hits with
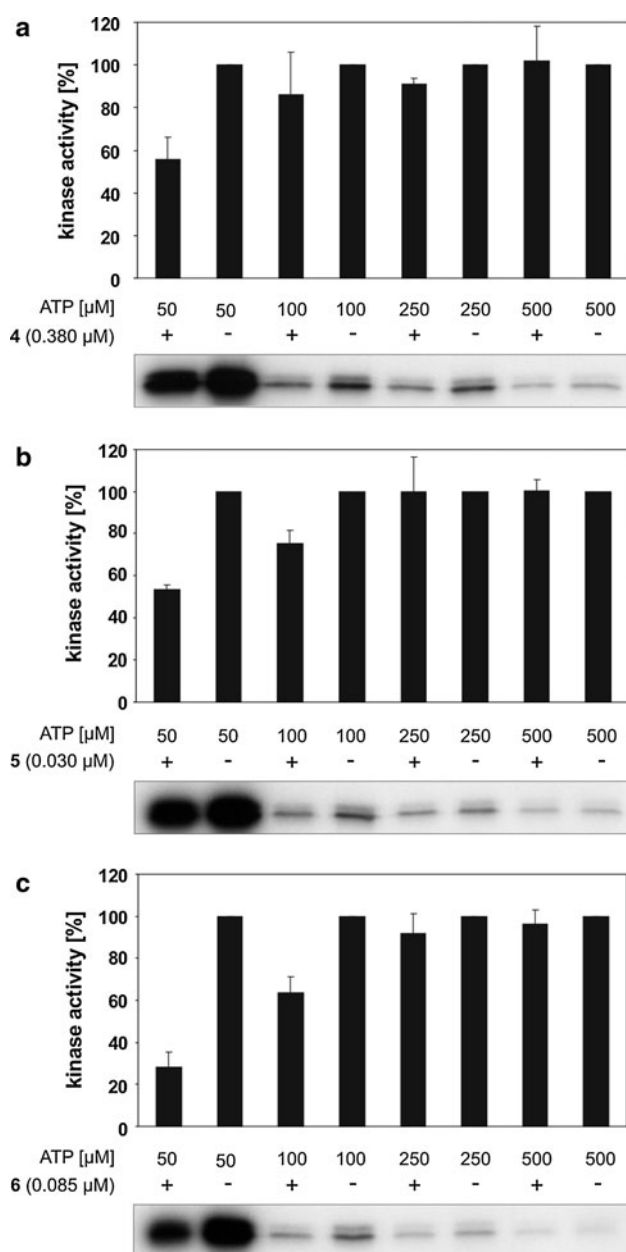
Fig. 6 Compounds **4**, **5** and **6** inhibit CK1δ in an ATP competitive manner. Inhibitors **4** (**a**; 380 nM), **5** (**b**; 30 nM) and **6** (**c**; 85 nM) were assayed in the presence of the indicated ATP concentrations. Kinase assays were perfomed using CK1δkd as enzyme and GST-p53$^{1-64}$ fusion protein (FP267) as substrate. Kinase activity in reactions containing inhibitor was calculated relative to the control reaction for each ATP concentration. While ATP concentrations increase, incorporation of radioactive labeled phosphate into substrate FP267 decreases, leading to weakened signals in the autoradiographs

nanomolar activity. These compounds were piperidino-thiazole carboxylamido-benzimidazoles (Leban et al. 2007). The NFκB pathway is complex and contains many possible targets for inhibition. We therefore further investigated the mechanism of action of these compounds and established that

the inhibition of NFκB is derived from the multiple kinase inhibition profile.

To further improve the physicochemical properties of the series we deleted the piperidino part of the molecule and derived at acylaminobenzothiazolocarboxamidobenzothi-azoles as exemplified by compounds **1–10** in Table 1.

The compounds were tested in kinase assays using a CK1 specific substrate as described. The parent compound **9** had only moderate but significant effects on CK1δkd ($IC_{50} = 1.116$ μM). When the benzimidazole NH was replaced by S (as in compound **10**) or O (as in compound **11**), kinase activity was even more decreased. When the NH of the benzimidazole was blocked by methylation in compound **3** activity against CK1δkd was lost. An improvement of activity was obtained when a hydrophobic trifluoro-methyl residue was introduced into the benzimidazole in compound **5** (IC_{50} CK1δTV1 = 0.022 μM). Similarly, hydrophobic halogen residues in **6** lead to good activity with an IC_{50} of 0.048 μM for CK1δTV1. If one compares compound **5** with compounds **4** and **7** it is obvious that the trifluoromethoxyphenylacyl on the aminobenzothiazole is optimal. Hydrophylic groups on the benzimidazole as in compound **1** and **2** lead to diminished activity. The SAR presented is in good agreement with the X-ray structure results and fully explains most interactions found.

Although some isoform selective effects of the tested molecules could be observed, especially for compound **5** (up to 7-fold more active on CK1δkd compared to CK1ε), in the concentration range which is commonly used and necessary for cell-based screening and therapeutic application, isoform selectivity will not be observed. Being highly conserved within the kinase domain, the CK1 iso-forms significantly differ in their N- and C-terminal domains. According to our results inhibitory (auto-)phosphorylation within the C-terminal regulatory domain not only influences kinase activity but also the effect of inhibitor molecules. When kinase proteins are expressed for 14 h at 15°C C-terminal phosphorylation is reduced leading to increased kinase activity and more potent inhibitor action. Increased C-terminal phosphorylation comes along with less potent action of inhibitor molecules. This observation could be explained by inhibitor compounds competing with the C-terminal domain which can act as pseudo-substrate thereby possibly blocking the cat-alytic center of the kinase (Gietzen and Virshup 1999; Rivers et al. 1998).

According to the data obtained from the selectivity profiling also CK1 isoforms α and γ turned out to be targets of at least compound **5**. However, effects of the molecules presented in this study have not yet been tested on CK1α and γ.

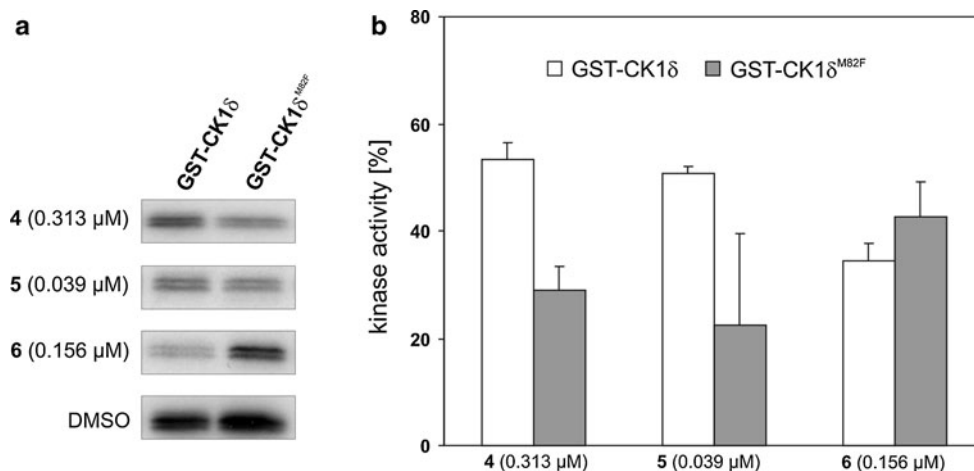For the three most effective compounds the postulated binding to the CK1δ protein was validated in vitro. The

Fig. 7 Inhibition of GST-wt CK1δ and a GST-CK1δ^{M82F} gatekeeper mutant. **a** Compounds **4** (0.313 μM), **5** (0.039 μM) and **6** (0.156 μM) were assayed for their ability to inhibit GST-wt CK1δ in comparison to a GST-CK1δ^{M82F} gatekeeper mutant using GST-p53$^{1-64}$ fusion protein (FP267) as substrate. GST-CK1δ^{M82F} shows stronger inhibition of kinase activity in the presence of compounds **4** and **5** and a lower inhibition in the presence of compound **6** than GST-wt CK1δ. **b** Kinase activity is presented as bar graph normalized towards solvent controls

Table 3 Docking free energy estimation for optimized and rescored protein-compound complexes in kcal/mol

Compound no.	**4**	**5**	**6**	**6**b
wt CK1δ	−30.2	−32.8	**−32.9**	**−34.1**
CK1δ^{M82F}	**−31.2**	**−33.3**	−30.2	−32.8

first approach clearly confirmed the ATP competitive properties of the tested compounds since inhibitory effects are disappearing along with increasing ATP concentration. The second approach, using the CK1δ^{M82F} gatekeepe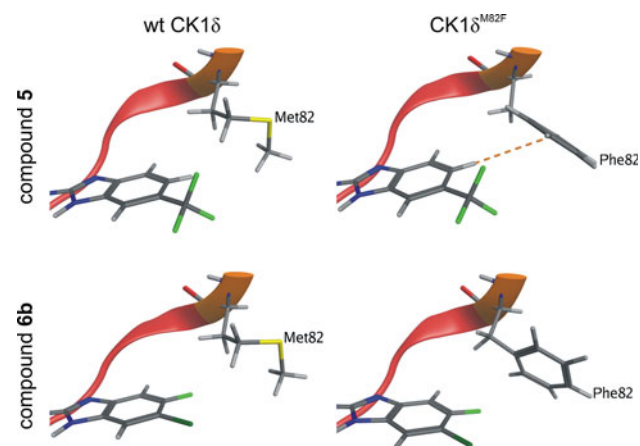r mutant, is some more sophisticated. The ATP binding site is highly conserved among most protein kinases. However, access of the ligand to the hydrophobic binding pocket can be tightly controlled by various gatekeeping amino acid residues. If these residues get mutated, substrate phosphorylation and also inhibitor action can be affected (Elphick et al. 2007). In the case of rat CK1δ the gatekeeping residue is methionine 82 which was mutated to the more bulky phenylalanine in order to "close the gate" to the kinase's selectivity pocket (Oumata et al. 2008; Peifer et al. 2009). According to our predictions and X-ray models, the tested compounds are not occupying the selectivity pocket. Therefore, in spite of the "closed gate", **4** and **5** inhibited the activity of CK1δ^{M82F} better than that of wt CK1δ because of an additional π-hydrogen bond to phenylalanine 82.

In a final biological screen we demonstrated, that compounds **5** and **6** are able to negatively affect the proliferation of several tumor cell lines. Although our cell cycle analysis shows significant effects, we have to take into account that isoforms of the CK1 family of protein kinases are involved in numerous cellular signalling pathways. Thus consideration of the cellular background is crucial for evaluation of any results. In order to get a more detailed insight to affected

Fig. 8 Interaction differences of **5** and **6b** in wt CK1δ and the CK1δ^{M82F} gatekeeper mutant Exemplary docking poses of compounds **5** (*top*) and **6b** (*bottom*) in wt CK1δ (*left*) and CK1δ^{M82F} (*right*). The hinge-region is marked *red* and the gatekeeper *orange*. The π-hydrogen bonds discerning the compounds in inihibition strength are *dotted orange*

Fig. 9 Cell cycle analysis of selected cell lines after treatment with ▶ compounds **5** and **6** Cell cycle analysis of Frwt648, mKSA, Colo357 and OVCAR-3 cells treated with compounds **5** and **6** (2 or 4 μM) for 48 h. Cells were stained with propidium iodide and analyzed using a flow cytometer. Control cells were treated with DMSO. The SV40-transformed Frwt648 and mKSA cells were highly sensitive towards treatment with **5** and **6**. Additionally to the increased amount of dead cells treatment of Colo357 also resulted in more cells in G1 phase of the cell cycle and treatment of OVCAR-3 also slightly increased the amount of cells in G2 phase
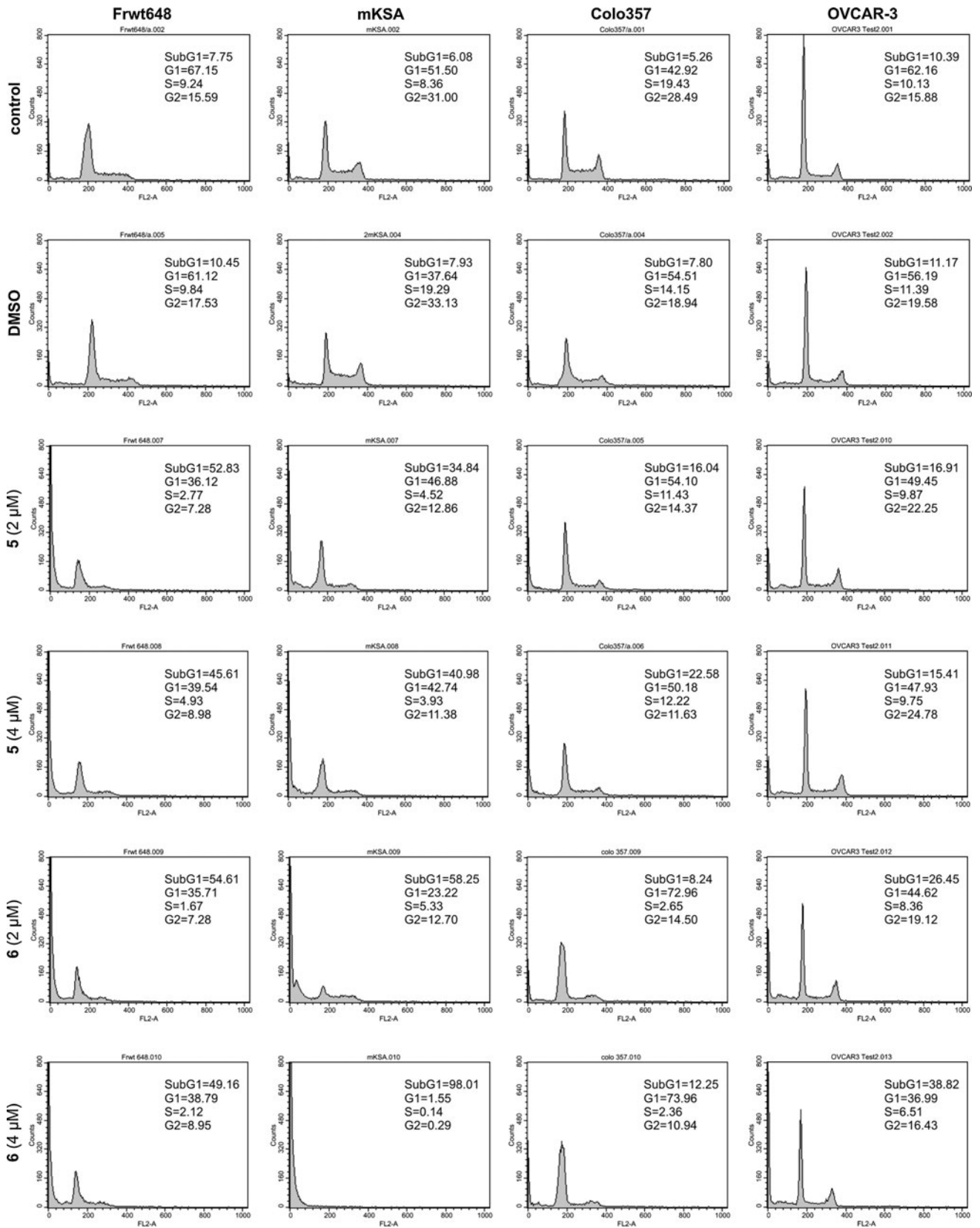
cellular pathways and functions, more complex approaches for cell culture based profiling are needed.

In conclusion we designed and characterized new inhibitor compounds with remarkable selectivity towards CK1δ and ε.

References

Baghdiguian S, Martin M, Richard I, Pons F, Astier C, Bourg N, Hay RT, Chemaly R, Halaby G, Loiselet J, Anderson LV, Lopez de Munain A, Fardeau M, Mangeat P, Beckmann JS, Lefranc G (1999) Calpain 3 deficiency is associated with myonuclear apoptosis and profound perturbation of the IkappaB alpha/NF-kappaB pathway in limb-girdle muscular dystrophy type 2A. Nat Med 5(5):503–511. doi:10.1038/8385

Bamborough P, Morse MA, Ray KP (2010) Targeting IKKbeta for the treatment of rheumatoid arthritis. Drug News Perspect 23(8):483–490. doi:10.1358/dnp.2010.23.8.1447844

Cheong JK, Virshup DM (2010) Casein kinase 1: complexity in the family. Int J Biochem Cell Biol 43(4):465–469. doi:10.1016/j.biocel.2010.12.004

Collaborative Computational Project (1994) The CCP4 suite: programs for protein crystallography. Acta Crystallogr D Biol Crystallogr 50(Pt 5):760–763. doi:10.1107/S0907444994003112

Criswell LA (2010) Gene discovery in rheumatoid arthritis highlights the CD40/NF-kappaB signaling pathway in disease pathogenesis. Immunol Rev 233(1):55–61. doi:10.1111/j.0105-2896.2009.00862.x

Demer L, Tintut Y (2011) The roles of lipid oxidation products and receptor activator of nuclear factor-kappaB signaling in atherosclerotic calcification. Circ Res 108(12):1482–1493. doi:10.1161/CIRCRESAHA.110.234245

Elphick LM, Lee SE, Gouverneur V, Mann DJ (2007) Using chemical genetics and ATP analogues to dissect protein kinase function. ACS Chem Biol 2(5):299–314. doi:10.1021/cb700027u

Giamas G, Hirner H, Shoshiashvili L, Grothey A, Gessert S, Kuhl M, Henne-Bruns D, Vorgias CE, Knippschild U (2007) Phosphorylation of CK1delta: identification of Ser370 as the major phosphorylation site targeted by PKA in vitro and in vivo. Biochem J 406(3):389–398. doi:10.1042/BJ20070091

Gietzen KF, Virshup DM (1999) Identification of inhibitory autophosphorylation sites in casein kinase I epsilon. J Biol Chem 274(45):32063–32070

Gil A, Maria Aguilera C, Gil-Campos M, Canete R (2007) Altered signalling and gene expression associated with the immune system and the inflammatory response in obesity. Br J Nutr 98(Suppl 1):S121–S126. doi:10.1017/S0007114507838050

Gill C, Walsh SE, Morrissey C, Fitzpatrick JM, Watson RW (2007) Resveratrol sensitizes androgen independent prostate cancer cells to death-receptor mediated apoptosis through multiple mechanisms. Prostate 67(15):1641–1653. doi:10.1002/pros.20653

Hamilton TC, Young RC, McKoy WM, Grotzinger KR, Green JA, Chu EW, Whang-Peng J, Rogan AM, Green WR, Ozols RF (1983) Characterization of a human ovarian carcinoma cell line (NIH:OVCAR-3) with androgen and estrogen receptors. Cancer Res 43(11):5379–5389

Hinzpeter M, Deppert W (1987) Analysis of biological and biochemical parameters for chromatin and nuclear matrix association of SV40 large T antigen in transformed cells. Oncogene 1(2):119–129

Kit S, Kurimura T, Dubbs DR (1969) Transplantable mouse tumor line induced by injection of SV40-transformed mouse kidney cells. Int J Cancer 4(4):384–392

Knippschild U, Milne D, Campbell L, Meek D (1996) p53 N-terminus-targeted protein kinase activity is stimulated in response to wild type p53 and DNA damage. Oncogene 13(7):1387–1393

Knippschild U, Milne DM, Campbell LE, DeMaggio AJ, Christenson E, Hoekstra MF, Meek DW (1997) p53 is phosphorylated in vitro and in vivo by the delta and epsilon isoforms of casein kinase 1 and enhances the level of casein kinase 1 delta in response to topoisomerase-directed drugs. Oncogene 15(14):1727–1736

Knippschild U, Gocht A, Wolff S, Huber N, Lohler J, Stoter M (2005a) The casein kinase 1 family: participation in multiple cellular processes in eukaryotes. Cell Signal 17(6):675–689. doi:10.1016/j.cellsig.2004.12.011

Knippschild U, Wolff S, Giamas G, Brockschmidt C, Wittau M, Wurl PU, Eismann T, Stoter M (2005b) The role of the casein kinase 1 (CK1) family in different signaling pathways linked to cancer development. Onkologie 28(10):508–514. doi:10.1159/000087137

Leban J, Baierl M, Mies J, Trentinaglia V, Rath S, Kronthaler K, Wolf K, Gotschlich A, Seifert MH (2007) A novel class of potent NF-kappaB signaling inhibitors. Bioorg Med Chem Lett 17(21):5858–5862. doi:10.1016/j.bmcl.2007.08.022

Leibovitz A, Stinson JC, McCombs WB 3rd, McCoy CE, Mazur KC, Mabry ND (1976) Classification of human colorectal adenocarcinoma cell lines. Cancer Res 36(12):4562–4569

Li H, Malhotra S, Kumar A (2008) Nuclear factor-kappa B signaling in skeletal muscle atrophy. J Mol Med (Berl) 86(10):1113–1126. doi:10.1007/s00109-008-0373-8

Li X, Su J, Cui X, Li Y, Barochia A, Eichacker PQ (2009) Can we predict the effects of NF-kappaB inhibition in sepsis? Studies with parthenolide and ethyl pyruvate. Expert Opin Investig Drugs 18(8):1047–1060. doi:10.1517/13543780903018880

Lin L, Peng SL (2006) Coordination of NF-kappaB and NFAT antagonism by the forkhead transcription factor Foxd1. J Immunol 176(8):4793–4803 pii: 176/8/4793

Mashhoon N, DeMaggio AJ, Tereshko V, Bergmeier SC, Egli M, Hoekstra MF, Kuret J (2000) Crystal structure of a conformation-selective casein kinase-1 inhibitor. J Biol Chem 275(26):20052–20060. doi:10.1074/jbc.M001713200

Milne DM, Palmer RH, Campbell DG, Meek DW (1992) Phosphorylation of the p53 tumour-suppressor protein at three N-terminal sites by a novel casein kinase I-like enzyme. Oncogene 7(7):1361–1369

Morgan RT, Woods LK, Moore GE, Quinn LA, McGavran L, Gordon SG (1980) Human cell line (COLO 357) of metastatic pancreatic adenocarcinoma. Int J Cancer 25(5):591–598

Murshudov G, Vagin A, Dodson E (1996) Application of Maximum Likelihood Refinement. Proceedings of Daresbury Study Weekend 4

Nichols D, Chmiel J, Berger M (2008) Chronic inflammation in the cystic fibrosis lung: alterations in inter- and intracellular

signaling. Clin Rev Allergy Immunol 34(2):146–162. doi:
10.1007/s12016-007-8039-9

Oumata N, Bettayeb K, Ferandin Y, Demange L, Lopez-Giral A,
Goddard ML, Myrianthopoulos V, Mikros E, Flajolet M, Green-
gard P, Meijer L, Galons H (2008) Roscovitine-derived, dual-
specificity inhibitors of cyclin-dependent kinases and casein
kinases 1. J Med Chem 51(17):5229–5242. doi:10.1021/jm8001
09e

Pargellis C, Tong L, Churchill L, Cirillo PF, Gilmore T, Graham AG,
Grob PM, Hickey ER, Moss N, Pav S, Regan J (2002) Inhibition
of p38 MAP kinase by utilizing a novel allosteric binding site.
Nat Struct Biol 9(4):268–272. doi:10.1038/nsb770

Peifer C, Abadleh M, Bischof J, Hauser D, Schattel V, Hirner H,
Knippschild U, Laufer S (2009) 3,4-Diaryl-isoxazoles and
-imidazoles as potent dual inhibitors of p38alpha mitogen
activated protein kinase and casein kinase 1delta. J Med Chem
52(23):7618–7630. doi:10.1021/jm9005127

Perez DI, Gil C, Martinez A (2010) Protein kinases CK1 and CK2 as
new targets for neurodegenerative diseases. Med Res Rev
31(6):924–954. doi:10.1002/med.20207

Peterson JM, Guttridge DC (2008) Skeletal muscle diseases, inflam-
mation, and NF-kappaB signaling: insights and opportunities for
therapeutic intervention. Int Rev Immunol 27(5):375–387. doi:
10.1080/08830180802302389

Price MA (2006) CKI, there's more than one: casein kinase I family
members in Wnt and Hedgehog signaling. Genes Dev
20(4):399–410. doi:10.1101/gad.1394306

Rasheed S, Nelson-Rees WA, Toth EM, Arnstein P, Gardner MB
(1974) Characterization of a newly derived human sarcoma cell
line (HT-1080). Cancer 33(4):1027–1033

Rena G, Bain J, Elliott M, Cohen P (2004) D4476, a cell-permeant
inhibitor of CK1, suppresses the site-specific phosphorylation
and nuclear exclusion of FOXO1a. EMBO Rep 5(1):60–65. doi:
10.1038/sj.embor.7400048

Rivers A, Gietzen KF, Vielhaber E, Virshup DM (1998) Regulation
of casein kinase I epsilon and casein kinase I delta by an in vivo
futile phosphorylation cycle. J Biol Chem 273(26):15980–15984

Stone KR, Mickey DD, Wunderli H, Mickey GH, Paulson DF (1978)
Isolation of a human prostate carcinoma cell line (DU 145). Int J
Cancer 21(3):274–281

Wei J, Feng J (2010) Signaling pathways associated with inflamma-
tory bowel disease. Recent Pat Inflamm Allergy Drug Discov
4(2):105–117 pii: BSP-IAD-2009-4

Wolff S, Xiao Z, Wittau M, Sussner N, Stoter M, Knippschild U
(2005) Interaction of casein kinase 1 delta (CK1 delta) with the
light chain LC2 of microtubule associated protein 1A (MAP1A).
Biochim Biophys Acta 1745(2):196–206. doi:10.1016/j.bbamcr.
2005.05.004